

ACCEPTED MANUSCRIPT • OPEN ACCESS

Internal Short Circuit Analysis of Cylindrical Lithium-Ion Cells Due to Structural Failure

To cite this article before publication: Muhammad Sheikh *et al* 2021 *J. Electrochem. Soc.* in press <https://doi.org/10.1149/1945-7111/abec54>

Manuscript version: Accepted Manuscript

Accepted Manuscript is “the version of the article accepted for publication including all changes made as a result of the peer review process, and which may also include the addition to the article by IOP Publishing of a header, an article ID, a cover sheet and/or an ‘Accepted Manuscript’ watermark, but excluding any other editing, typesetting or other changes made by IOP Publishing and/or its licensors”

This Accepted Manuscript is © 2021 The Author(s). Published by IOP Publishing Ltd..

As the Version of Record of this article is going to be/has been published on a gold open access basis under a CC 4.0 licence, this Accepted Manuscript is available for reuse under the applicable CC licence immediately.

Everyone is permitted to use all or part of the original content in this article, provided that they adhere to all the terms of the applicable licence referred to in the article – either <https://creativecommons.org/licenses/by/4.0/> or <https://creativecommons.org/licenses/by-nc-nd/4.0/>

Although reasonable endeavours have been taken to obtain all necessary permissions from third parties to include their copyrighted content within this article, their full citation and copyright line may not be present in this Accepted Manuscript version. Before using any content from this article, please refer to the Version of Record on IOPscience once published for full citation and copyright details, as permissions may be required. All third party content is fully copyright protected and is not published on a gold open access basis under a CC licence, unless that is specifically stated in the figure caption in the Version of Record.

View the [article online](#) for updates and enhancements.

Internal Short Circuit Analysis of Cylindrical Lithium-Ion Cells Due to Structural Failure

Journal:	<i>Journal of The Electrochemical Society</i>
Manuscript ID	JES-103091.R1
Manuscript Type:	Research Paper
Date Submitted by the Author:	25-Jan-2021
Complete List of Authors:	Sheikh, Muhammad; University of Warwick, WMG Elmarakbi, Mohab; Northumbria University, Mechanical and construction engineering Rehman, Sheikh; University of Sunderland, Engineering Elmarakbi, Ahmed; Northumbria University, Mechanical and construction engineering
Keywords:	Batteries – Li-ion, Energy Storage, Degradation, Short circuit, finite element analysis, quasi static load

SCHOLARONE™
Manuscripts

Accepted Manuscript

Internal Short Circuit Analysis of Cylindrical Lithium-Ion Cells Due to Structural Failure

Muhammad Sheikh,^{1,z} Mohab Elmarakbi,² Sheikh Rehman,³ and Ahmed Elmarakbi²

¹WMG, the University of Warwick, Coventry CV4 7AL, United Kingdom

²Department of Mechanical and Construction Engineering, Faculty of Engineering and Environment, Northumbria University, Newcastle NE18ST, United Kingdom

³University of Sunderland, Faculty of Technology, Sunderland SR6 0DD, United Kingdom

^zE-mail: muhammad.sheikh@warwick.ac.uk

Abstract:

Battery failures are obvious after being subject to abuse conditions however predicting these failures in advance is crucial when using test and validation techniques to understand battery potential. Lithium-ion battery cells are widely used due to their high energy and power densities. When abusive conditions like the three point bend loading are applied to lithium-ion batteries, what occurs to the mechanical behaviours and components is still mostly unknown. To further this understanding, this paper investigates the mechanical behaviour of the separator in the LiCoO₂/Graphite cylindrical 18650 cells. Internal short circuit (ISC) behaviour, strain rate dependency and electrochemical status of the cells (i.e. SOC dependency) are studied to understand failure pattern. Furthermore, simple and effective constitutive model for the separator layer is formed, facilitating further mechanical analysis and numerical simulation of lithium-ion battery study. Occurrence of ISC is investigated by jellyroll deformation where casing is removed, and quasi-static load is applied. Numerical simulation model is developed to further investigate sequential structural failures and temperature changes. Simulation results showed good accuracy with experimental results and are useful to predict structural failure of cells. Number of failures including electrolyte leakage, change in shape, sudden voltage drop/temperature rise, and gas venting are observed.

1. Introduction

The growth of the electric vehicle industry is required to help circumvent pollution and ensure emission control. Which is why it is expected that 50% of world's passenger vehicles will be electric by 2050 [1]. With any new technology, it is important to identify

1
2
3 potential challenges and be able to address them. The main areas of focus now are
4 powertrain architecture, propulsion systems, control systems and design. With regards
5 to propulsion systems the electric vehicle uses lithium-ion batteries which allows it to
6 propel with great performance whilst having a long lifetime [2]. However, there are
7 always risks associated with battery technology that can be mitigated to improve
8 safety. Standard tests procedures are also available to test batteries with minimizing
9 risks where to characterise a lithium-ion battery, different testing techniques are used
10 [3-5]. Some of the methods used, employ advanced equipment and tools including
11 universal battery testers, advanced power supplies, accelerating rate calorimeter
12 (ARC) [3],[6], thermal chambers, IR thermography and high resolution cameras. Some
13 of these techniques are combined with basic lab-based techniques, including
14 characterisation at different charging and discharging rates, variation of applied
15 current and voltages, capacity estimation at different operating temperatures and cell
16 temperature estimation using thermocouples [6-8]. When it comes to short circuit
17 study, it becomes a challenging task to consider these limitations. The purpose of an
18 abuse test is to study and understand the lithium-ion battery's failure pattern and its
19 mechanisms of failure. This paper studies the three-point bend mechanical loading
20 condition and the associated failure patterns.
21
22
23
24
25
26
27
28
29
30
31
32
33

34
35 The short circuit phenomenon of the lithium-ion battery can be divided into various
36 types but in general, is divided as internal short circuit (ISC) or external short circuit
37 (ESC). When cell terminals are shorted together outside the battery this refers to
38 external short circuit whilst internal short circuit (ISC) develops inside the cell. ISC can
39 be further divided into various types depending on the location and contact area. In [9]
40 authors provided statistics of internal and external short circuits and documented that
41 occurrence of ISC due to vehicle collision is 52% whereas occurrence of ESC is 26%.
42 Causes of ESC and ISC are different but over the period, they can result in similar
43 failure patterns. ESC is often a result from a vehicle collision, battery pack or cell
44 leakage, rollover and abusive operating conditions. For instance, abnormal
45 charge/discharge and operating temperatures. On the other hand, ISC development
46 is more complicated. In [10] authors provided three types of ISC which are: mechanical
47 abuse caused by damage/deformation of separator due to crushing, thermal abuse
48 caused by the collapse of a separator due to excessive temperature and electrical
49 abuse where separator failure occurs as a result of dendrite growth due to overcharge
50
51
52
53
54
55
56
57
58
59
60

1
2
3 or over discharge [11-14]. The focus of this study is on mechanical and thermal abuse
4 analysis of separator layers.
5

6
7 Various mechanical abuse conditions are considered for ISC study and it was found
8 that the type of loading has a great impact on failure pattern and severity [15]. The
9 most common type of loading condition used for short circuit studies are nail
10 penetration, three-point bend, side impact and compression. All of the loading
11 conditions can cause failure or damage to the separator, anode and cathode, which
12 can result in irreversible ISC [16]. Some Immediately notable failure patterns
13 documented by [17-20] are sudden voltage drops, temperature rise, electrolyte
14 leakage, venting gas and chemical decomposition reactions, which can lead to thermal
15 runaway or permanent damage to the battery.
16
17

18
19 In [21-23] various loading conditions are discussed, however a full understanding of
20 loading-dependent and electrochemical-dependent mechanical behaviours of lithium-
21 ion battery components is essential for battery safety, optimization and evaluation [24].
22

23
24 A Significant amount of work is done to understand cell failure at the micro and macro
25 scales. We are only discussing micro scale failures and the initiation of those failures
26 within this work. Saharei et al., [25-27] has conducted a series of experiments to
27 understand the failure patterns of cylindrical cells and the evolution of stress using dog
28 bone specimens. In [28], authors investigated the fracture analysis of particles on
29 current collectors using the diffusion of lithium ions during charging and discharging
30 [29]. In [30], authors explained that the expansion of cathode/anode particles would
31 cause grain fractures leading to battery capacity deterioration or sudden failure [31].
32 In [32], the authors reported that the charge/discharge would cause the exfoliation and
33 failure of the SEI membrane [33] as well as the adhesive failure due to the electrode
34 volume change [34]. In addition, the volume change of electrodes due to
35 intercalation/de-intercalation can introduce extra stress within the battery [35].
36 Although these all provide extensive failure information due to ISC, the fact remains
37 that to recreate sequential failure is still a challenging task. Current studies primarily
38 focus on the mechanical abusive conditions and analysis of ISC. For ISC initiation, nail
39 penetration tests are widely conducted where voltage and temperature variations are
40 studied to understand battery failures, but due to the unknown nature of impact, it is
41 necessary to study various shapes and sizes of indenter. Three-point bend loading
42
43
44
45
46
47
48
49
50
51
52
53
54
55
56
57
58
59
60

1
2
3 conditions create brutal failure scenarios, which range from fracture, buckling, rupture
4 or breaking of the cell. This study will investigate these avenues in detail as well as
5 the mechanical aspects of separator failure due to three-point bend loading therefore
6 the published work related to deep electrochemistry including electrolyte leakage or
7 damage to inner core is not discussed. ISC linking to mechanical and thermal abuse
8 is further discussed where a numerical simulation approach is used to replicate these
9 failures for the further study of the material properties. Finite element analysis (FEA)
10 methods are commonly used by [25-28 & 36-41], which allows for the evaluation of
11 the mechanical properties of battery specimens. This evaluation occurs where material
12 properties are known, or sensitivity analysis can be used to determine these
13 properties. In addition, lumped jellyroll models are considered to study failure patterns,
14 but layer stacks are not considered, and individual material properties are not detailed.
15 In [25] authors replicated fracture study using numerical simulation when temperature
16 distribution across the layer is not considered. Within this paper, we have considered
17 cell stacks with layer properties. Due to the limitation of electromagnetic (EM) solvers,
18 electrochemistry is not included in the simulation work and failures reported are a
19 result from the mechanical and thermal solver. The role of testing batteries for early
20 detection of performance discrepancies for electric vehicle (EV) application has
21 encouraged the investigation of this significant issue in detail.

22
23
24
25
26
27
28
29
30
31
32
33
34
35
36
37
38
39
40
41
42
43
44
45
46
47
48
49
50
51
52
53
54
55
56
57
58
59
60
In this paper failure analysis is conducted where two states of charge (SOCs)
conditions (0% and 75%) are considered to analyse ISC of cylindrical 18650 cells.
Separator failure criterion is used for further investigation of electrochemical failures
where stress-strain and voltage-temperature relation is studied.

2. Experimental setup

Low capacity cells are chosen to avoid severe conditions during cell conditioning and
actual tests. These cells have a steel casing of thickness ~0.30mm and spiral wound
layers of the: anode, cathode, separator, anode current collector and cathode current
collector.

Three-point bend test is performed on 18650 lithium-ion cells to check the mechanical
integrity of these cells, to show where the cells bend when most of the stress is exerted
on the mid bottom surface. Three-point bend tests are not commonly used for these

types of batteries, and very little evidence was found in [24-26] and [42], where the type of indenter and support varied in dimensions. Three-point bend test holder and indenter dimensions are given in table 1.

Description	dimensions
Cell holder length	88mm
Cell holder width	56mm
Cell holder cuts	19.7mm
Bottom rigid plate thickness	4mm
Gap between holder plates	42mm
Indenter length	7.4mm
Indenter thickness	1mm
Indenter length	24.5mm
Rod diameter	11.70mm

Table 1: Three-point bend indenter and holder dimensions

A Sharp edge with a thickness 1 mm is selected for this study as it differs from the nail penetration tests. Whilst carrying out the study, sudden loading conditions were calculated which could be the result of initial deformation of the separator layers. On the other hand, it could be the result of current collectors coming into contact and due to the energy absorption after short circuit forces drops down to low values and impact becomes quasi-static. Experimental set up is shown in figure 1.

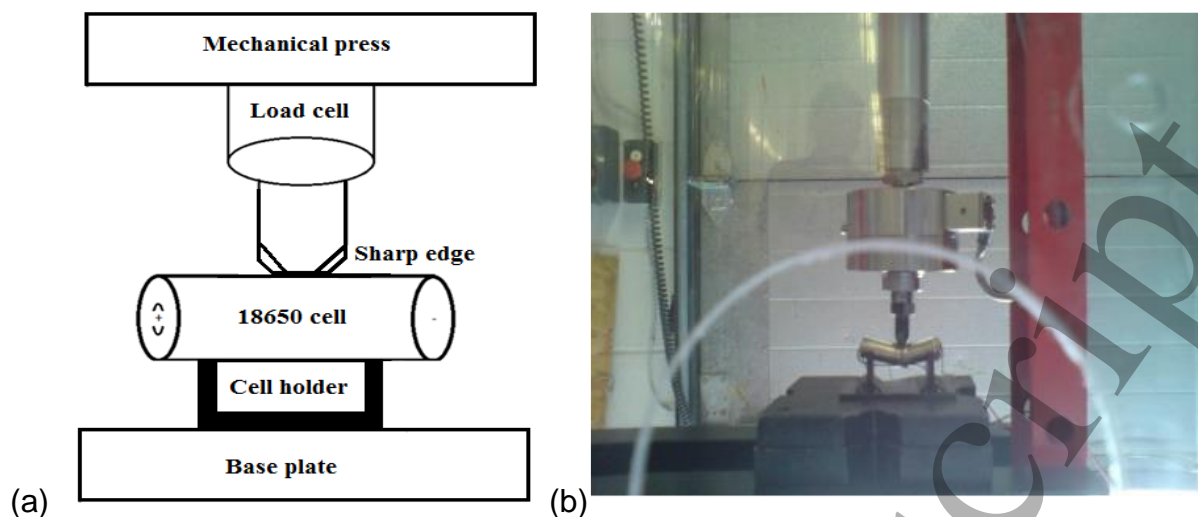


Figure 1: (a) Line diagram for Three-point test, (b) Experimental setup for Three-point bend test

The Maximum force required to initiate a short circuit for 75% SOC is 2.98 kN, however lower force values are recorded at 0% SOC. Both a temperature increase and voltage drop were recorded for the two tests as shown in figure 2.

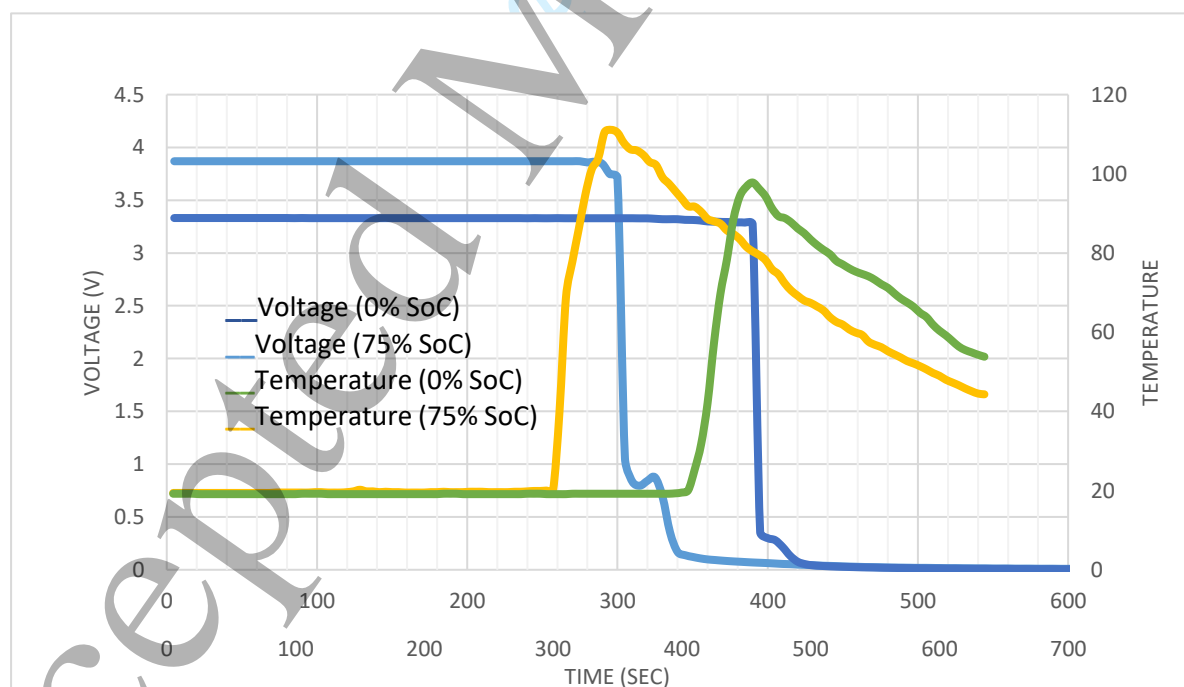
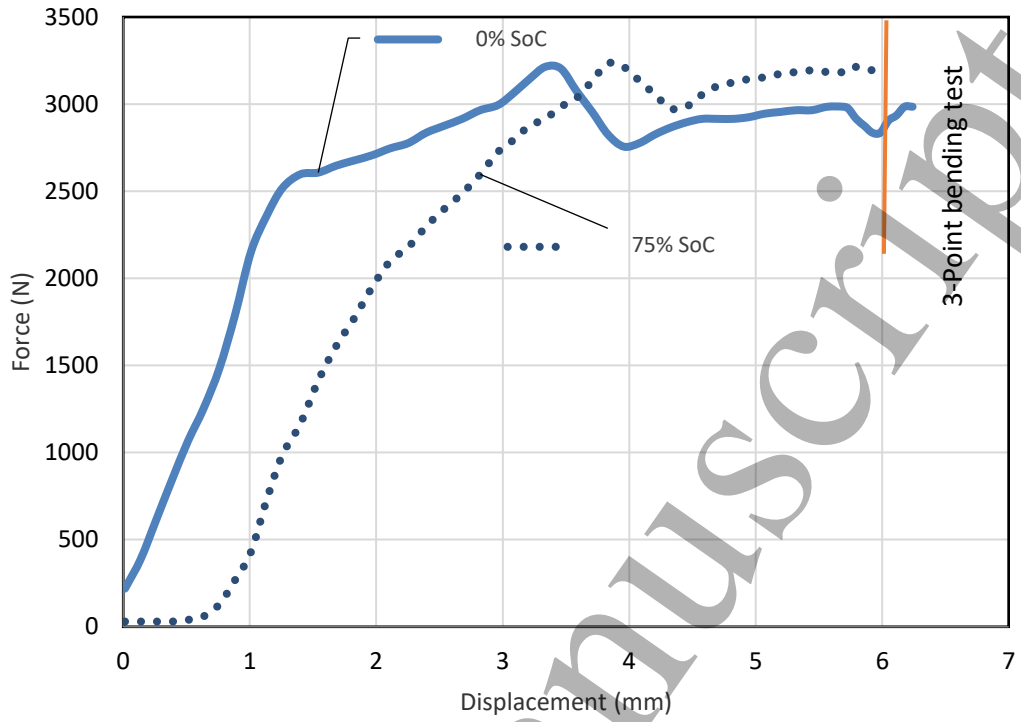
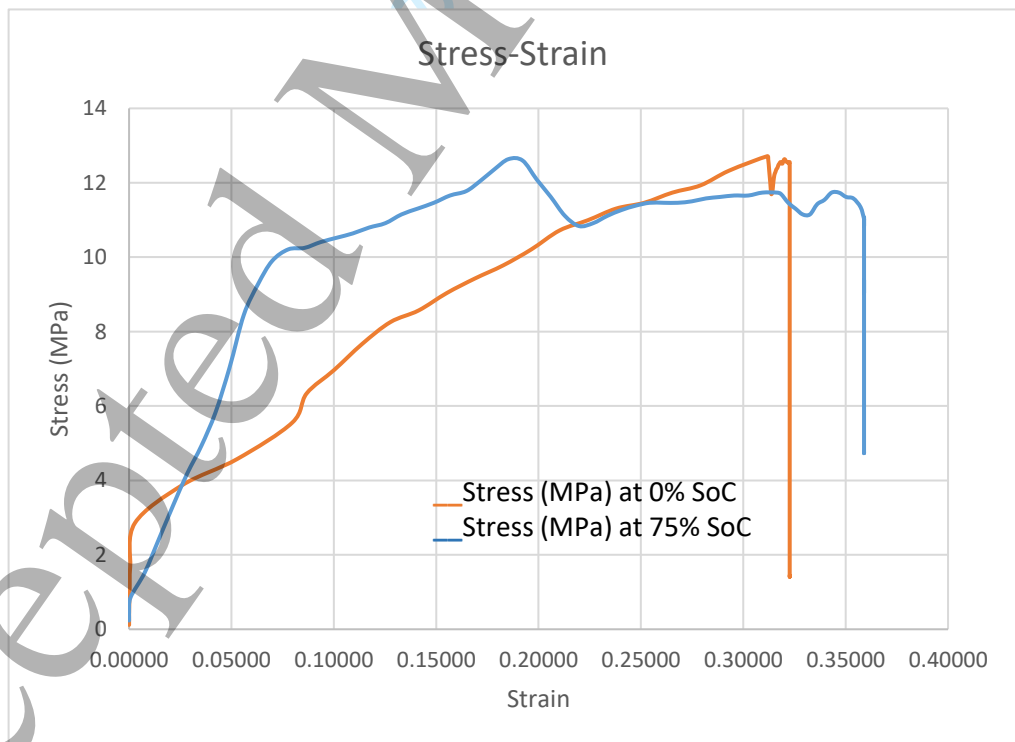


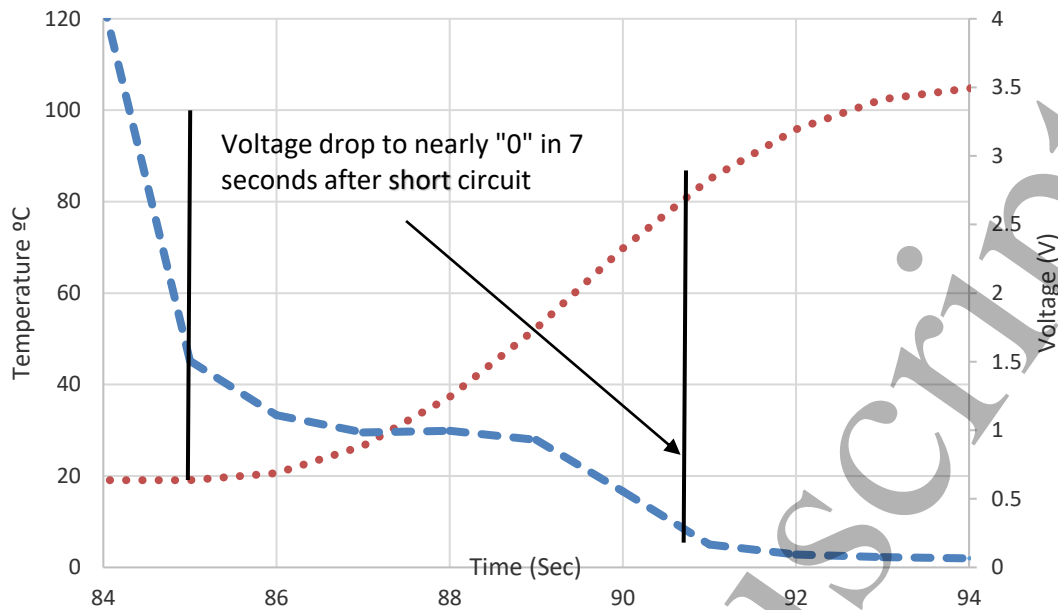
Figure 2: Voltage and temperature relation at the time of failure



(a)



(b)



(c)

Figure 3: (a) Three-point bend test, Force and displacement relation at 0% and 75% SOC, (b) Stress-Strain relation, (c) Sudden voltage drop as a result of short circuit due to bending

Temperature rise was sudden and rose at the rate of $700^{\circ}\text{C}/\text{minute}$. Sharp edge cracks occurred on the sides and mid surface as well as tension occurring at the bottom which showed the stiffness of the steel material at the time of impact. Similar results were observed for 0% SOC and 75% SOC. As shown in figure 3, initially the cell experienced an elastic region, but fractures occurred at a force of 2.5kN for 0% SOC and at 3.2kN the cell started to undergo deformation which is the initiation of ISC for this test. 75% more force was required for the initial fracture, which was 3.2kN, and permanent deformation occurred immediately after the initial fracture at 3kN and the cell experienced a short circuit. The buckling of the steel casing was observed when the force varied due to the softening of the steel casing but did not achieve permanent deformation [42].

As explained above, a short circuit occurrence will be slow within high SOC cells, but temperature variation will be high due to the high-energy storage content. Rate of temperature change may vary depending on many factors including, area of the fracture and position of temperature measurement. In figure 3(c), voltage drop due to

a short circuit is shown and it was observed that it took 7 seconds to attain the voltage drop to nearly zero value following the high temperatures attained. For three-point bend test, nominal stress and nominal strain behaviour were calculated using equations 1 to 4 as follows [21].

$$\sigma_n = \frac{F}{A} \quad (1)$$

Where F is the force applied as shown and discussed in this chapter and previous chapters, A is the area of contact which is given by [42] as follows,

$$A = l_c b_c \quad (2)$$

Where l_c is the length of the cell and width of the contact b_c , is calculated by Eq. 4.5, as given below,

$$b_c = 2R \arccos \left[\frac{R-s/2}{R} \right] \quad (3)$$

Where "R" is the radius of the cell and "s" is the displacement of the indenter used, so the nominal strain ϵ_n can be obtained using Eq. 4.6, given as follow

$$\epsilon_n = \frac{s}{2R} \quad (4)$$

All the analysis mentioned in this section are discussed with each test protocol in the following section and the conclusion of the analysis is presented in the later section.

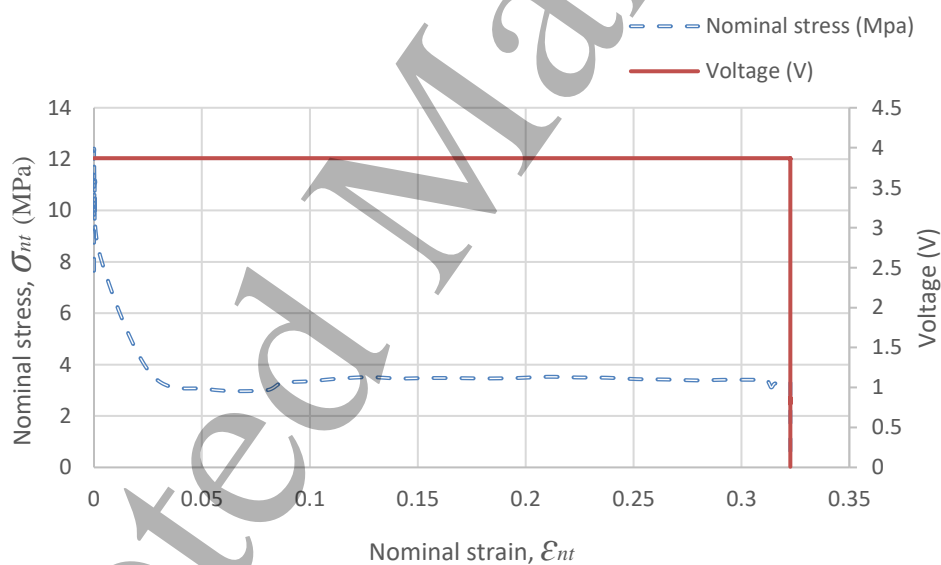
2.1 Immediate failure analysis

Sharp edge indenter is used to investigate sharp object effect on cylindrical cells and possible thermal runaway events. At force (F_{t0}) which was 2.33kN a short circuit occurred during the 0% SOC test, where the complete discharge of the cell took 110 sec. Short circuit displacement (d_{st0}) was 6.46mm, and temperature change (ΔT_{t0}) was 16.3°C. Table 2, gives the values of the parameters observed during the impact test.

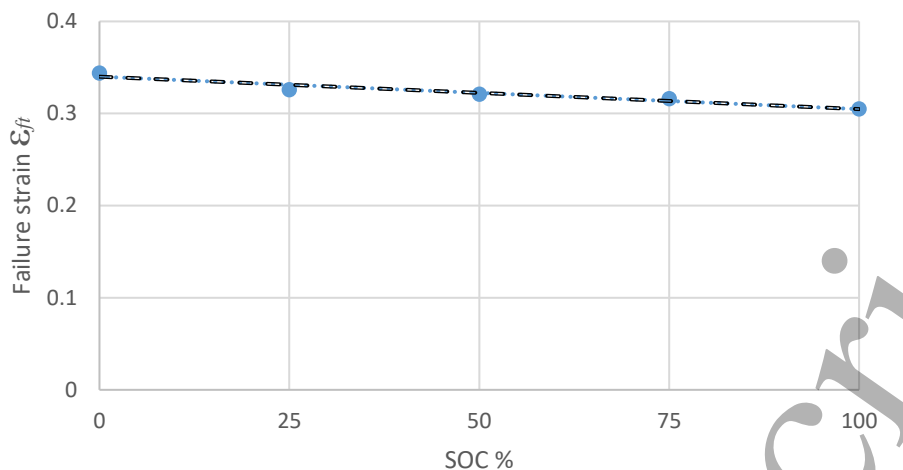
SoC	Time (Sec) t_r	Force (KN) F_r	Displacement (mm) d_{sr}	Initial temp (°C) T_{ir}	Final temp (°C) T_{fr}	Change in temp (°C) ΔT_r	Voltage V_r	Nominal failure Strain ϵ_{nr}	Nominal failure stress, σ_{nr} (MPa)
0%	280	10.32	8.389	20.0	25.30	5.30	3.343	0.4661	8.754
75%	310	12.25	6.971	21.3	107.5	86.20	3.894	0.3870	11.490

Table 2: Rod test results at short circuit development

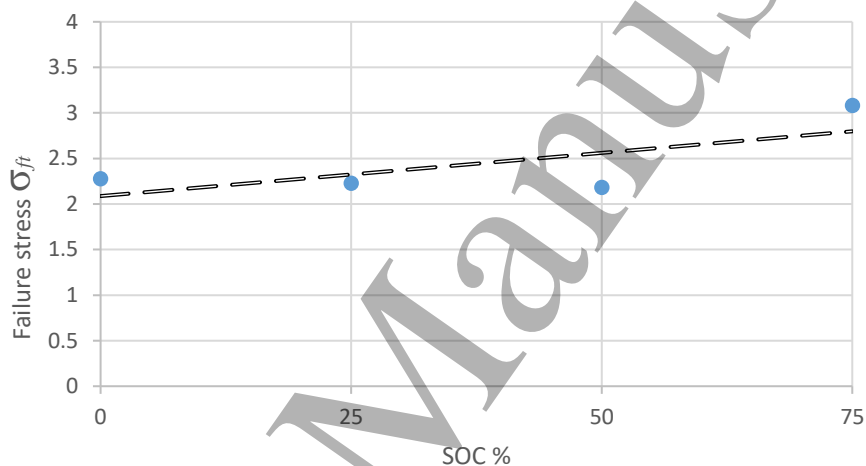
2.2 Nominal stress-strain analysis



(a)



(b)



(c)

Figure 4: (a) Three-point bend test, Nominal stress-strain and voltage-strain curve, (b) Nominal failure strain for three-point bend test, (c) Nominal failure stress for three-point bend test

As shown in figure 4(a), nominal stress and nominal strain for battery degradation in the three-point bend test were observed where ϵ_{nt} represented nominal strain for three-point bend test, and σ_{nt} represented nominal stress for three-point bend test. In regard to the case of battery bending test it indicates that the initial high-stress values were due to the steel casing buckling which in turn penetrates deep into the layers and failure across the layers occurs. To better understand and generalise cell failure due to bending, failure strain for the three-point bend test is shown in figure 4(b).

$$\varepsilon_{ft} = 0.34 - 0.0004SOC \quad (5)$$

Eq. (5) shows linear fit for the three-point bend test where ε_{ft} represents failure strain for the three-point bend test. Eq. (5) has adjusted R square fit of 0.9384. As can be seen in figure 6, strain failure for the three-point bend test has linearly decreasing function where at lower SOC high strain failure was observed.

Figure 4(c), shows failure stress for the three-point bend test which is unlike the failure strain which was high at low SOC. Linear fit for failure stress is given in Eq. (6), where σ_{ft} represents failure stress for three-point bend test.

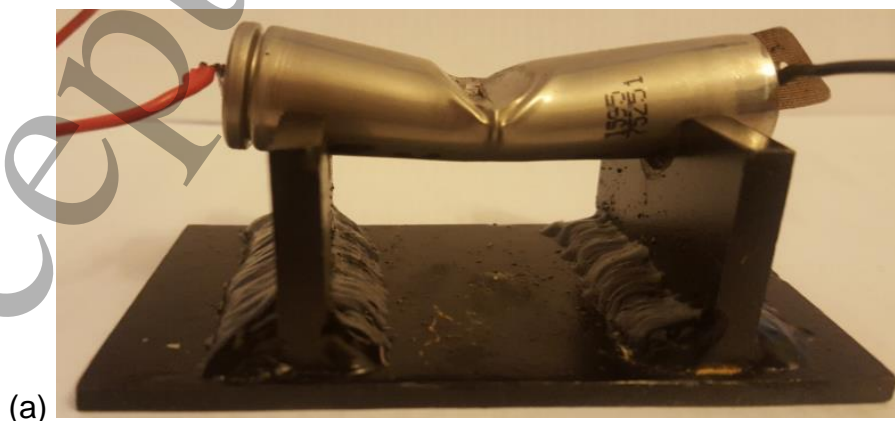
$$\sigma_{ft} = 2.0872 + 0.0095SOC \quad (6)$$

2.3 Post-failure structural analysis

During the three-point bend test, cell bending and rupture was observed when the cell bent gradually. However, the formation of cracks was observed when the sharp edges were established in contact with the cell, shown in figure 5(a). Both cell fracture and buckling takes place in the three-point bend test when the sharp edge indenter is used. Cell terminals and end caps are intact in this testing; however, cell thinning took place at the centre of the cell. In this test, the indenter travelled 40% of original cell diameter where mean displacement is 7.27mm.

Sideway deflection can be observed in the three-point bend, which is due to the triangular shape of the indenter tip. At cell failure, the fracture is observed in the three-point bend test where drastic temperature and voltage variations are observed.

2.4 Post-failure temperature analysis



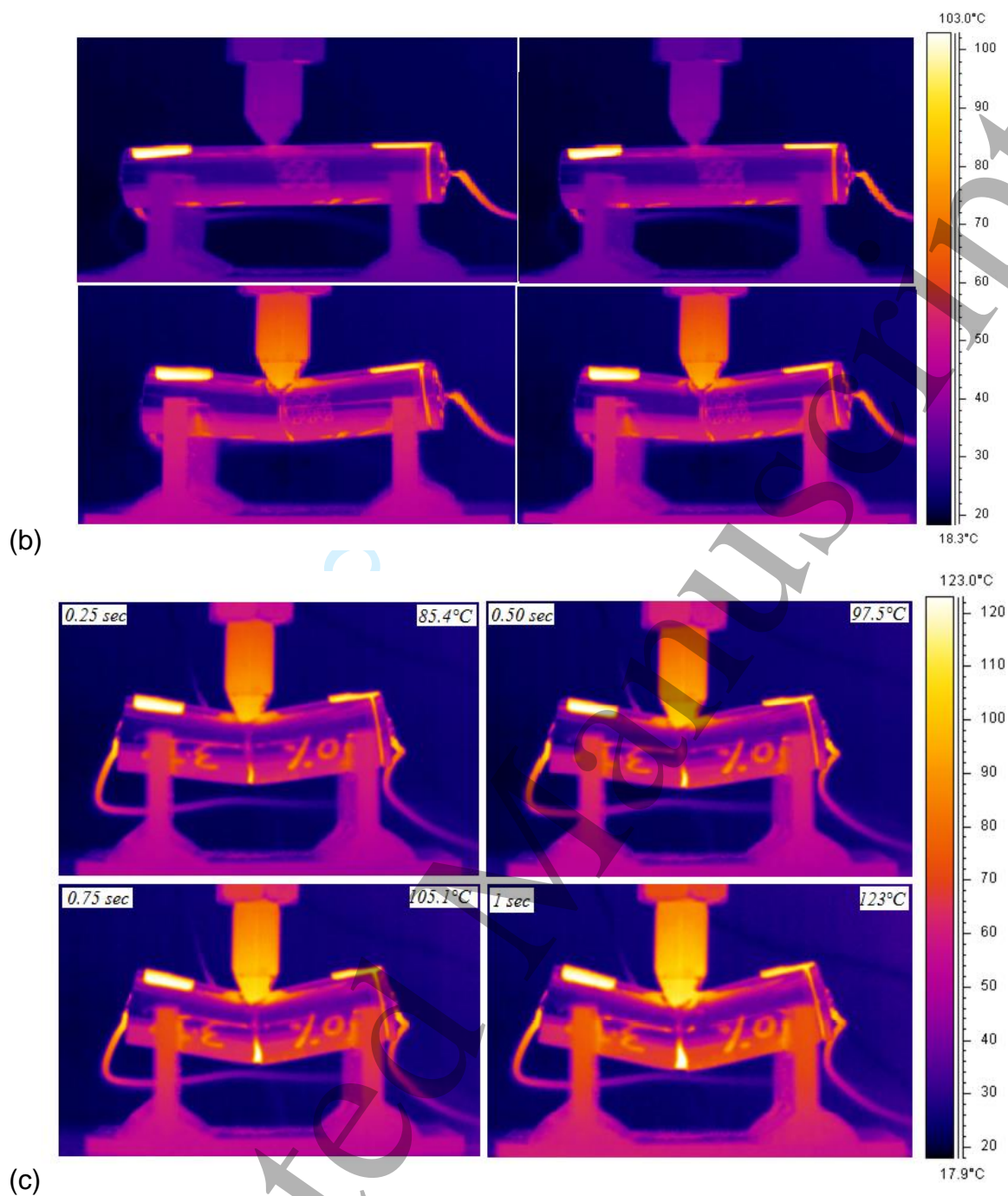


Figure 5: (a) Three-point bend test, (b) Initial results of temperature change for three-point bend test, (c) Initial temperature change with sample time for three-point bend test

75% SOC is chosen for further analysis where high-temperature change (ΔT_{t75}) and short circuit failure time (t_{t75}) are observed. In the figure 5(b), hotspot development is very slow and spans the period of time. The Hot spot is located at the bottom of the

1
2
3 cell where temperature change was observed for 1sec and heat dissipation effect is
4 negligible.
5
6

7
8 In figure 5(c), sample time with the temperature at the hotspot is shown, where the
9 high-temperature location located at the bottom mid of the cell, unlike commonly
10 reported bending and fracture pattern for the three-point bend test. Due to the indenter
11 shape the cell showed fractures on the top surface and bending at the bottom.
12
13

14
15 Cylindrical 18650 lithium-ion battery's homogeneous jellyroll models are found in the
16 current literature, which addresses the battery failures for quasi-static and dynamic
17 simulations. However detailed layered models, which are equally important to
18 understand sequential failures due to mechanical loading conditions, are not found in
19 detail. Within this paper battery layered models are developed using LS-DYNA
20 simulation tool and the results are validated.
21
22
23
24
25

26 27 **3. Validation of experimental results**

28
29 A layered battery model is chosen. The purpose of choosing an alternative model is
30 to verify results on a small scale compared to the lithium-ion cell model where the
31 number of elements is much higher which increases computation time. Making it
32 sometimes difficult to rectify issues if a complete cell model is encountered comprised
33 of several settings and conditions. For the initial model mainly three material types are
34 used, where for the separator, anode and cathode MAT_63_CRUSHABLE_FOAM is
35 used. A crushable foam material is used as it has an option of tension cut off where
36 tension is treated as elastic-perfectly-plastic at the tension cut-off value [43]. Detailed
37 validation of crushable foam is given by [44]. For the current collectors and steel
38 casing MAT_24_PIECEWISE_LINEAR_PLASTICITY is used. Piecewise linear
39 plasticity material model accounts for stress-strain behaviour where a curve can be
40 used to provide stress-strain values. For the rigid base plate, MAT_20_RIGID is used
41 to turn the solid element part into a rigid body. Detailed properties and relevant
42 characteristics of materials used can be found in LS-DYNA material model manual
43 [45]. Element size selection is crucial which affects computation efficiency as well as
44 stability of the model. Material properties for current collectors and active materials are
45 used from [45-49] and experimental study, which are given in table 3.
46
47
48
49
50
51
52
53
54
55
56
57
58
59
60

Material	Mass density (Tonne/mm ³)	Modulus of elasticity (MPa)	Poisson ratio	Yield stress (MPa)	% Failure strain ϵ_f
Copper current collector	7.94e-9	1.1e5	0.35	210	5
Aluminum current collector	2.69e-9	7e4	0.36	180	5
Anode	2.23e-9	1e4	0.3	100	10
Cathode	4.20e-9	1e4	0.3	100	10
Separator	1.179e-9	3.45e3	0.35	18	25
Steel casing	7.83e-9	2e5	0.3	450	4
Rigid plate	----	----	----	----	

Table 3: Material properties used for LS-DYNA simulation [46-51]

3.1 Formation of concentric layered model

In [52] authors mentioned 304 layers for 18650 cell which accounts for 38 stacks, where each stack contains eight layers. To model 304 layers with exact thickness requires high computation efficiency and modelling time, where very thin layers need special modelling precautions. Within this research, concentric layer-model formation was used to model 18650 cylindrical cell, which was not found in the literature, however, jellyroll model where all the layers are lumped in the jellyroll model was proposed by [26]. As cells have a spiral wound formation in general, a concentric layer model represents a different structure, where the main aim is to find an alternative way to model the battery where each layer is independent in regards of geometry. However, layers share mechanical and thermal behaviour under loading conditions. A thicker layer model is found to be the best choice to represent cells with the number of layers [48-50].

In this paper all layers are considered to be the same size, this assumption provides an opportunity for simplifying the model as well as, due to the low thickness compared to [48],[49] more layers can be integrated to form a complete cell. The Steel casing has an almost similar size to the original cell. Concentric layers can be an appropriate alternative to spiral wound layers, which are complex to design and simulate due to the different thicknesses of the cell layers.

3.2 Simulation parameters and assumptions

The initial cell temperature selected was 22°C, which is in agreement with single cell testing standards and SAEJ2464 standard, which sets the limit of 55°C for module level test. The battery model is modelled with fully integrated solid element formulation, where a total of 103306 elements are used. The size of elements for steel casing is 0.5mm and for all other layers is 1mm. The reason for different element size selection is to achieve accuracy, where steel housing is the first layer to experience load. All indenters and bottom plates are modelled as rigid geometry, where the rigid material MAT_20_RIGID was used. A coefficient of friction between cell and support is considered to be 0.3 as given by in [25]. No endcaps were taken into account for this simulation, however, SPC boundary conditions were used to restrain components of the battery if required. Failure strain of the separator documented by [49] was 93%; however, separator failure strain of 35% to 80% from the literature is evident, which means values of 0.2 to 0.5 (50% or 80% of initial thickness) could be used for the separator. Consistent units by (LSD-DYNA consistent units) were used for all simulation models given in table 4.

Consistent units (Steel material)							
Mass	Length	Time	Force	Stress	Energy	Density	Young's Modulus
<i>ton</i>	<i>mm</i>	<i>s</i>	<i>N</i>	<i>MPa</i>	<i>N-mm</i>	<i>(Tonne/mm³)</i>	<i>MPa</i>

Table 4: LS-DYNA consistent units

3.3 Cylindrical 18650 cell simulation model

Based on the above-mentioned properties and assumptions, the simulation model is designed to understand loading impact on the cell for separator failure analysis. For simulation, all layers (steel shell casing, anode, cathode, separators, anode current collector and cathode current collector) were considered to be 0.3mm thick and innermost radius was considered to be 1mm as detailed in [53]. It is important to understand the material properties for the individual layers for stress/strain relation and for that purpose, two foam material models were discussed in [26] and the three-point bend test was considered for the initial investigation. True stress/strain curve from the dogbone specimen for the shell casing is given and nominal failure stress and failure strain were used from the experimental results, where for each test case values at 0% SOC were used, which is to check if the model predicts failure. The steel casing material is modelled using MAT-24-PIECEWISE-LINEAR-PLASTICITY in LS-DYNA. The Separator, anode and cathode were considered to be as the MAT-63-CRUSHABLE-FOAM model, and the anode current collector and cathode current collector were modelled using MAT-003-PLASTIC-KINEMATIC. The stress/strain curve for the separator, active anode material and active cathode material were used from [49] and [53]. Coupled mechanical and thermal solver are used, where structural deformation is an input for the thermal solver. Heat capacity and thermal conductivity of individual layer along with the type of deformation contribute towards temperature variations of the cell.

Type of layer	Heat capacity ($Jkg^{-1}K^{-1}$)	Thermal conductivity ($Wm^{-1}K^{-1}$)
Steel shell casing	477	14.9
Separator	1978	0.334
Anode active material	700	5
Cathode active material	700	5
Anode current collector	386	400

Cathode current collector	900	200
---------------------------	-----	-----

Table 5: Cell heat capacity and thermal conductivity parameters for simulation

Boundary prescribed motion set is used in this simulation to define object motion throughout the simulation at every single time step. Due to the sensitive nature of contact cards, accurate contact interface modelling is necessary which improves finite element simulation results.

3.4 Three-point bend test simulation

For the three-point bend test simulation, cell holders and the sharp edge are modelled using rigid materials. Numerical simulation model for the three-point bend and experimental and simulation geometries for pre and post loading are shown in figure 6.

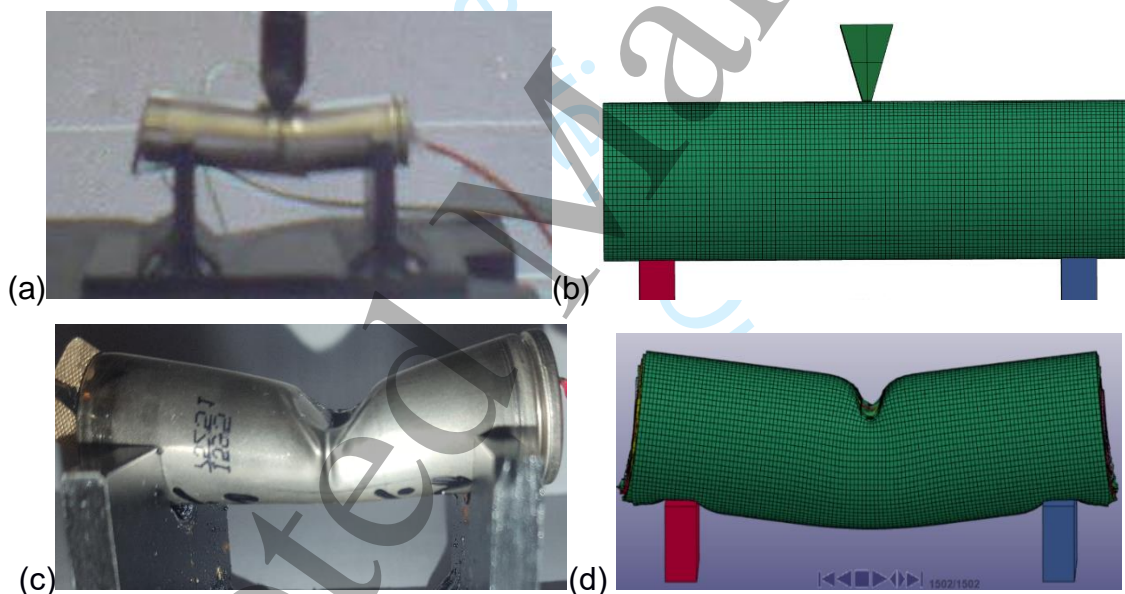


Figure 6: Three point bend test, (a) undeformed test, (b) undeformed simulation, (c) deformed test results quasi-static load, (d) deformed simulation result quasi-static load

Initially, when the load was applied on the cylindrical cell it used less force for compression but after some time due to the material hardening, excessive force was required for compression. Short circuit displacement was observed at 5.23mm for quasi-static analysis Figure 7 (a), shows resultant displacement due to quasi-static

loading.

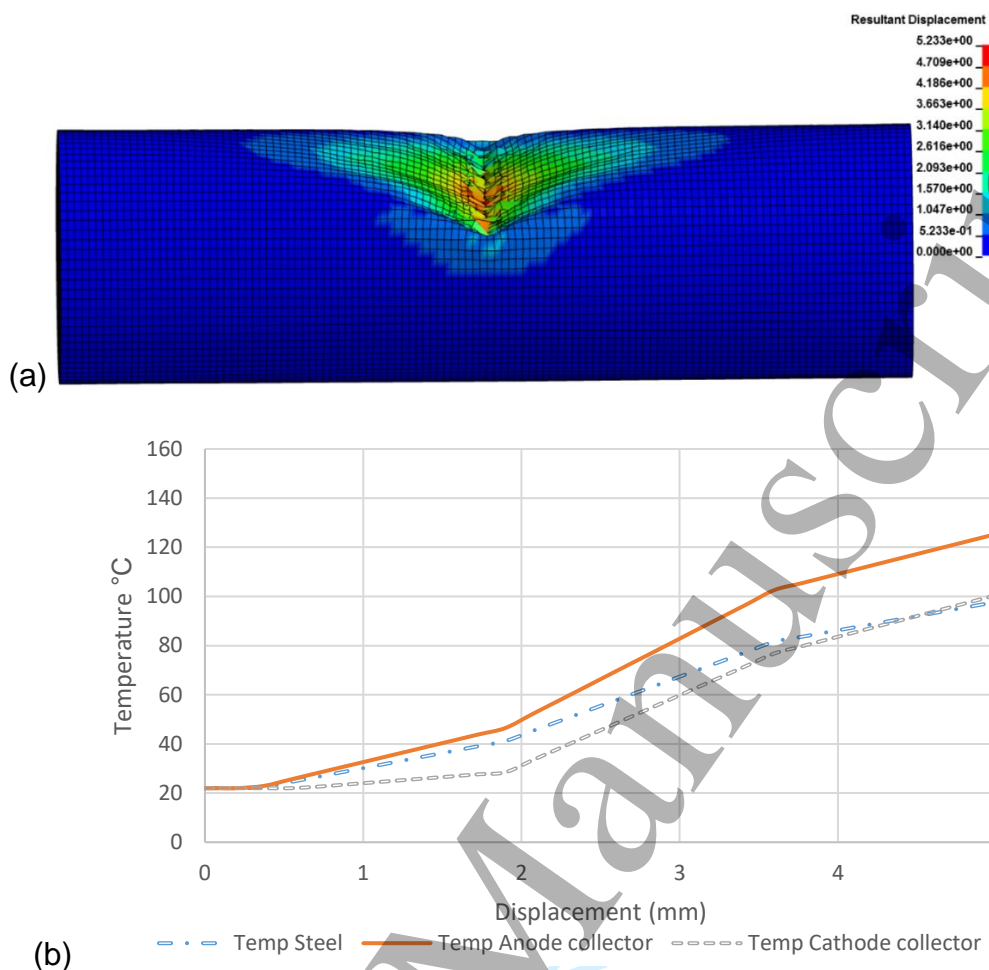


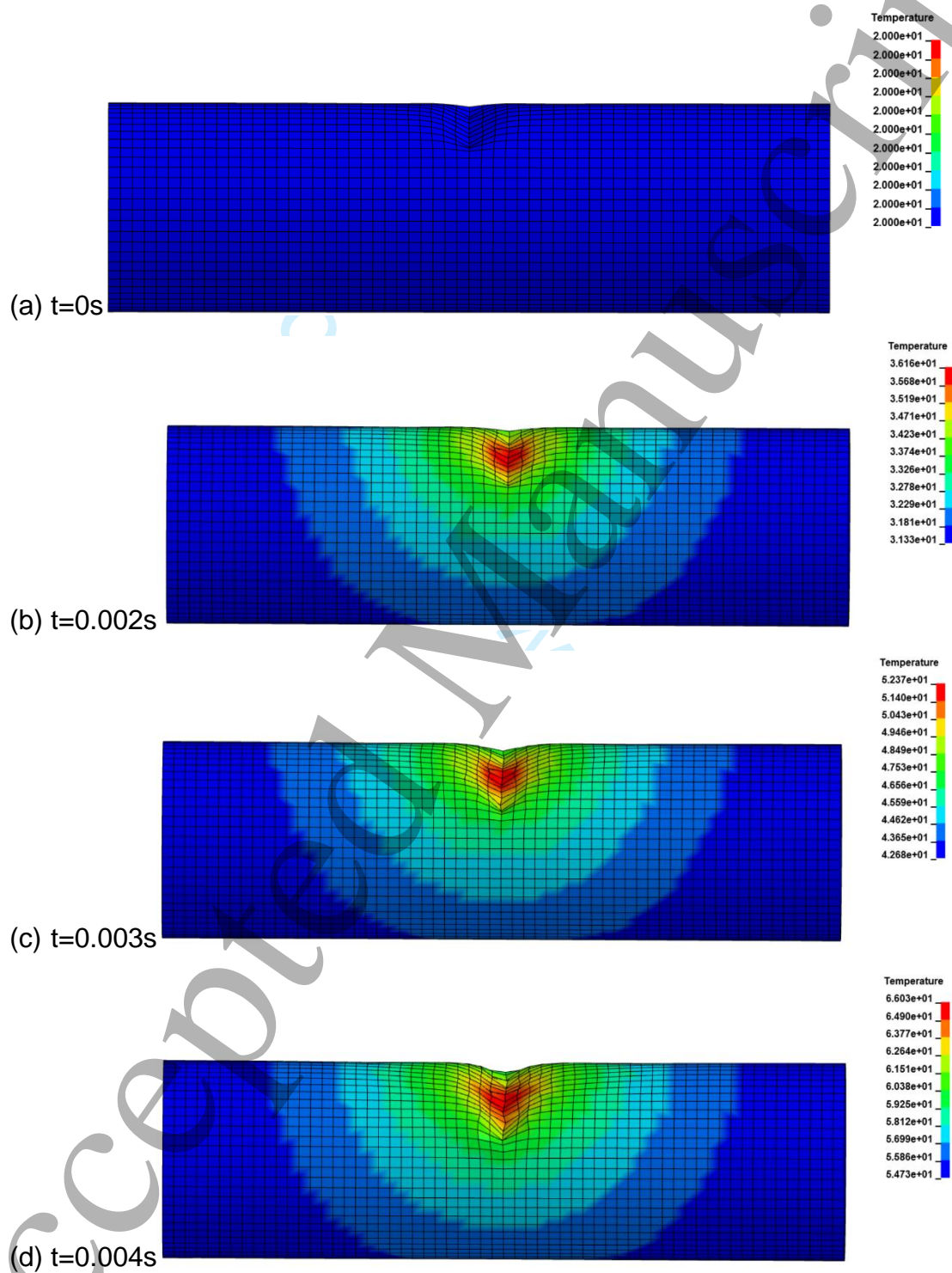
Figure 7: (a) Resultant displacement due to quasi-static load, (b) Temperature values for steel casing, anode current collector and cathode current collector

As can be seen from figure 7(a), sideways buckling of steel casing is found due to the sharp edge cell fracture is at the point of contact of sharp edge. For the three-point bend test simulation comparison of steel, anode current collector and cathode current collector layers are used to understand temperature distribution of the cell for the internal layers, where the anode current collector and cathode current collector indicates the first instance of short circuit. The negative electrode has a high thermal conductivity so the temperature change at the anode current collector is high compared to cathode current collector.

As can be seen from figure 7(b), temperature for the steel and cathode current collector (aluminium) is around 100°C; however temperature for the anode current collector is around 130°C at the time of short circuit occurrence.

3.5 Separator failure analysis

The three-point bend test short circuit failure was further analysed using a separator failure criteria, where all separator layers were examined for their temperature variations. Separator layer temperature variations are shown in figure 8.



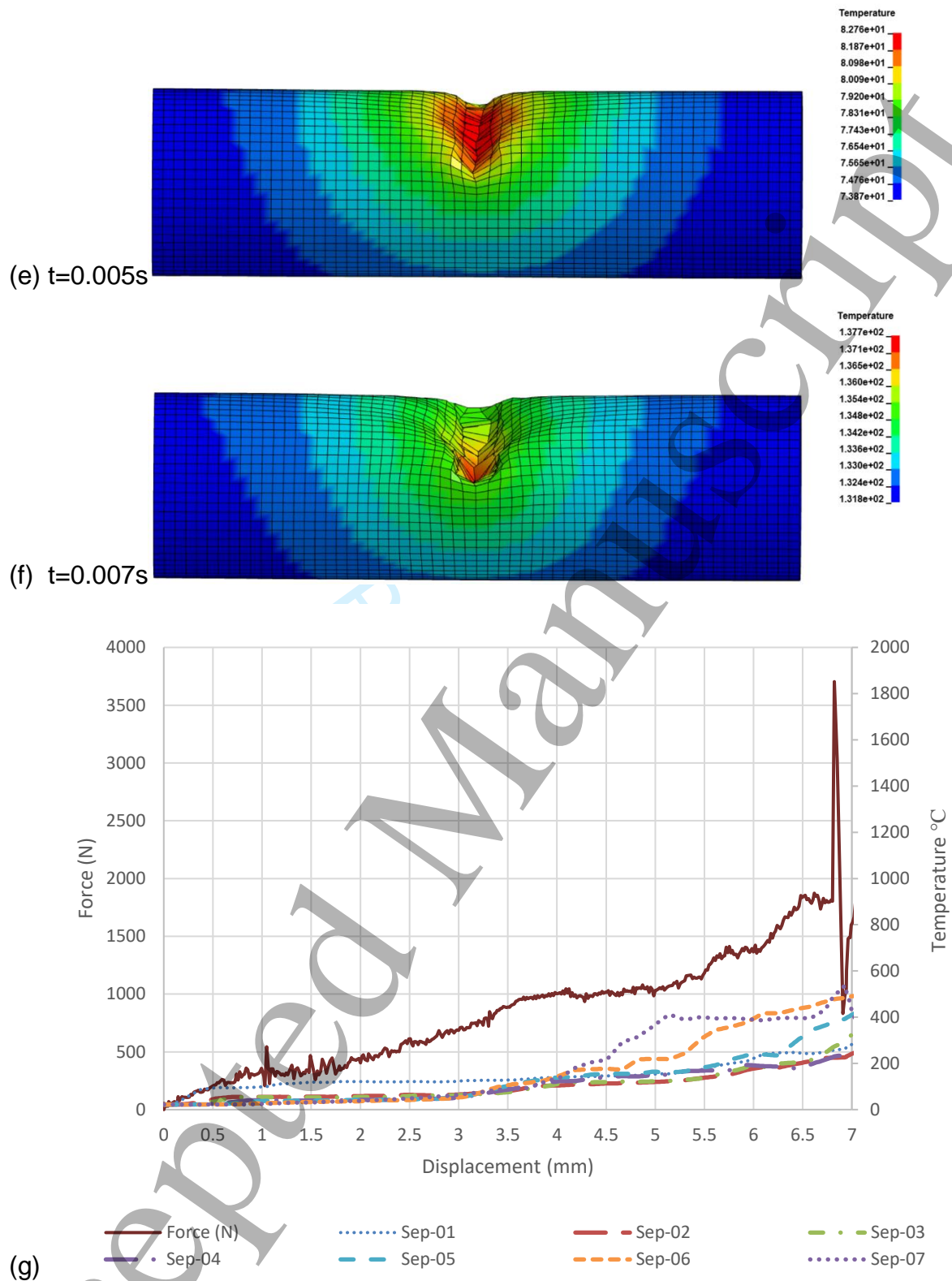


Figure 8: (a) to (f) Three point bend simulation, temperature variations at the first separator layer, (g) Separator layers behavior with applied force, displacement and temperature variations

1
2
3 The top surface of the separator layer 1, is shown for deformation and temperature
4 variation with regards to location. For separator layer 1, sideways deflection and
5 temperature variation is shown. Due to sharp-edge, cell damage occurs relatively early
6 compared to other loading cases, which sequentially damages layers within the cell.
7
8 Due to both the tension and compression separator layers having low mechanical
9 strength brittle fractures develops, which occurs immediately after the steel casing
10 fracture and temperature increases drastically as shown within the experiment work
11 and this simulation model. Layer behaviour due to the applied force is provided in
12 figure 8(b).
13
14
15
16
17
18

19 The simulation model results show good accuracy within the cell comparison. During
20 lithium-ion battery construction the separators have the lowest melting point and melts
21 at around 144°C [49], so separator failure will occur earlier compared to other layer
22 failure which have comparatively high melting points. This separator failure is also an
23 indication of ISC as contact between electrodes is established once separator layers
24 melt. As shown in figure 8(a) to 8(f), force attains the same peak value as documented
25 in the experimental section for the three-point bend, however a sudden drop in force
26 at around 7mm pinpoints the short circuit occurrence. The Temperatures of all layers
27 started to increase after short circuit and the last separator layer which is sep-07
28 experiences a temperature drop, which is stabilising zone or short circuit propagation.
29 Once the thermal runaway occurred temperature started to increase in an uncontrolled
30 manner, and temperature of all the layers were around 300°C except sep-05 to sep-
31 07 which attain temperatures of around 500°C for a short instance of time. Sep-07
32 layer experienced high compression and tension due to the three-point bend as forces
33 from all other layers and indenter were applied at this layer, where the layer shrinks
34 and element deletion takes place. Separator analysis with high-temperature variations
35 can be used as an indicator of ISC or initial cell failure.
36
37
38
39
40
41
42
43
44
45
46
47
48

49 **Conclusions**

50
51 Internal short circuit (ISC) behaviour, strain rate dependency and electrochemical
52 status of the cells (i.e. SOC dependency) are studied to understand failure pattern.
53 Occurrence of ISC is investigated by jellyroll deformation where casing is removed,
54 and quasi-static load is applied. Numerical simulation model is used to investigate
55 sequential structural failures and temperature changes. Simulation results showed
56
57
58
59
60

1
2
3 good accuracy with experimental results and are useful to predict structural failure of
4 cells. Immediate failures like electrolyte leakage, change in shape, sudden voltage
5 drop/temperature rise, and gas venting are observed. The Location and intensity of
6 short circuit, time for initial and complete failure of cells and structural deformation
7 were considered in detail as well as using simulation models to analyse separator
8 failures. One of the significant finding from this research is that at maximum
9 displacement separator temperature increased significantly and a drop in force was
10 observed. The time of short circuit and force drop was due to the internal stiffness of
11 layers where temperature started to increase, but high temperatures, which were
12 uncontrolled lead to severe failures. Another significant finding from separator layer
13 analysis is that there were high-temperature locations, which indicate electrochemical
14 changes due to internal short circuit. Furthermore, separator failure occurs well in
15 advance for short circuit for the three-point bend test, which has an immediate short
16 circuit response. Failure response of the separators is in agreement with the
17 experimental work where failure of the layers took place for the three-point bend, and
18 all separator layers showed high temperatures and changes in their shape.
19
20
21
22
23
24
25
26
27
28
29
30
31
32
33
34
35
36
37
38
39
40
41
42
43
44
45
46
47
48
49
50
51
52
53
54
55
56
57
58
59
60

References:

- [1] Abaza, Ahmed, Ferrari, Stefania, Wong, Hin Kwan, Lyness, Chris, Moore, Andrew D., Weaving, Julia, Blanco-Martin, Maria, Dashwood, Richard and Bhagat, Rohit (2018) Experimental study of internal and external short circuits of commercial automotive pouch lithium-ion cells. *Journal of Energy Storage*, 16 . pp. 211-217.
- [2] Dubarry, M., & Baure, G. (2020). Perspective on commercial Li-ion battery testing, best practices for simple and effective protocols. *Electronics* (Switzerland), 9(1). <https://doi.org/10.3390/electronics9010152>.
- [3] Sheikh, M., Elmarakbi, A., Rehman, S., A combined experimental and simulation approach for short circuit prediction of 18650 lithium-ion battery under mechanical abuse conditions, *Journal of Energy Storage* (2020) 32 101833.
- [4] Harlow, J. E., Ma, X., Li, J., Logan, E., Liu, Y., Zhang, N., Ma, L., Glazier, S. L., Cormier, M. M. E., Genovese, M., Buteau, S., Cameron, A., Stark, J. E., & Dahn, J. R. (2019). A Wide Range of Testing Results on an Excellent Lithium-Ion Cell Chemistry to be used as Benchmarks for New Battery Technologies. *Journal of The Electrochemical Society*. <https://doi.org/10.1149/2.0981913jes>.
- [5] Porcher, W., Montaru Cidetec Mikel Arrinda Martinez, M., Marongiu, A., Oyarbide Jülich Niloofar Ehteshami TU München Yao Wu HI Ulm Arianna Moretti, M. F., Passerini, S., & Jan Berckmans ViF Philip Kargl, G. (2017). Draft White Paper Test methods for improved battery cell understanding.
- [6] Ruiz, V., Pfrang, A., Kriston, A., Omar, N., Van den Bossche, P., & Boon-Brett, L. (2018). A review of international abuse testing standards and regulations for lithium ion batteries in electric and hybrid electric vehicles. In *Renewable and Sustainable Energy Reviews*. <https://doi.org/10.1016/j.rser.2017.05.195>.
- [7] Tomaszewska, A., Chu, Z., Feng, X., O'Kane, S., Liu, X., Chen, J., Ji, C., Endler, E., Li, R., Liu, L., Li, Y., Zheng, S., Vetterlein, S., Gao, M., Du, J., Parkes, M., Ouyang, M., Marinescu, M., Offer, G., & Wu, B. (2019). Lithium-ion battery fast charging: A review. *ETransportation*. <https://doi.org/10.1016/j.etrans.2019.100011>
- [8] Zhang, G., Cao, L., Ge, S., Wang, C. Y., Shaffer, C. E., Rahn, C. D., 2014. "In Situ Measurement of Radial Temperature Distributions in Cylindrical Li-Ion Cells". *Journal of the Electrochemical Society*, 161(10), pp. A1499–A1507.
- [9] Doughty, D., and Roth, E.P., 2012. "A General Discussion of Li-Ion Battery Safety". *The Electrochemical Society Interface*, summer 2012, pp.37-44.
- [10] Lu, L., Han, X., Li, j., Hua, J., Ouyang, M., 2013. "A review on the Key Issues for Lithium-ion Battery Management in Electric Vehicles". *Journal of Power Sources*, 226, pp. 272-288.
- [11] Budde-Meiwes, H., Drillkens, J., Lunz, B., Muennix, J., Rothgang, S., Kowal, J., Sauer, D.U., 2013. "A review of current automotive battery technology and future prospects". *Proceedings of the Institution of Mechanical Engineers, Part D: Journal of Automobile Engineering*, 227, 5, pp. 761 – 776.
- [12] Kizilel, R., Sabbah, R., Selman, J.R., Al-Hallaj, S., 2009. "An alternative Cooling System to Enhance the Safety of Li-Ion Battery Packs". *Journal of Power Sources*, 194, pp. 1105-1112.
- [13] Smith, K.A., Rahn, C.D., Wang, C.Y., 2007. "Control oriented 1D electrochemical model of lithium ion battery". *Energy Conversion and Management*, 48, 9, pp. 2565-2578.

- 1
2
3 [14] Julien, C., Mauger, A., Zaghib, K., Groult, H., 2016. "Optimization of Layered Cathode Materials
4 for Lithium-Ion Batteries". *Materials*, 9, pp. 595.
5
- 6 [15] He, H., Xiong, R., Guo, H., Li, S., 2012. "Comparison Study on the Battery Models used for Energy
7 Management of Batteries in Electric Vehicles". *Energy Conversion and Management*, pp. 113–121.
8
- 9 [16] Zhao, R., Gu, J., Liu, J., 2014. "An Investigation on the Significance of Reversible Heat to the
10 Thermal Behavior of Lithium Ion Battery through Simulations". *Journal of Power Sources*, 266, pp.
11 422–432.
12
- 13 [17] Albright, G., Al-Hallaj, S., 2012. "Making Lithium-ion Safe through Thermal Management".
14 <http://www.battcon.com/PapersFinal2012/Greg%20Albright%20->
15
- 16 [18] Lisbona, D., Snee, T., 2011. "A Review of Hazards Associated with Primary Lithium and Lithium-
17 ion Batteries". *Journal of Process Safety and Environmental Protection*, 89, pp.434-442.
18
- 19 [19] Shi, Y., Noelle, D.J., Wang, M., Le, A.V., Yoon H., Zhang M., Meng, Y., Qiao, Y., 2016.
20 1Exothermic Behaviors of Mechanically Abused Lithium-ion Batteries with Dibenzylamine". *Journal*
21 *of Power Sources*, 326, pp. 514-521.
22
- 23 [20] Miller J.M., 2009. "Energy Storage System Technology Challenges facing Strong Hybrid, Plugin
24 and Battery Electric Vehicles". *Proceedings of IEEE, Vehicle Power and Propulsion Conference, VPPC*
25 '09. 7-10 Sept. 2009, Dearborn, MI, USA.
26
- 27 [21] Sheikh, M., Elmarakbi, A., Elkady, M., 2017. "Thermal runaway detection of cylindrical 18650
28 lithium-ion battery under quasi-static loading conditions". *Journal of Power Sources*, 370, pp. 61–70.
29
- 30 [22] Sheikh, M., Elmarakbi, A., Rehman, S., 2020. "A combined experimental and numerical
31 simulation approach to predict short circuit due to mechanical abuse conditions", *Journal of Energy*
32 *storage*.
33
- 34 [23] Sheikh, M., Rehman, S., Elkady, M., 2018. "Numerical simulation model for short circuit
35 prediction under compression and bending of 18650 cylindrical lithium-ion battery". *Journal of Energy*
36 *Procedia*, Vol 151, Pages 187-193.
37
- 38 [24] Kim, G-H., Pesaran, A., Spotniz, R., 2007. "A Three Dimensional Thermal Abuse Model for
39 Lithium-Ion Cells". *Journal of Power Sources*, pp. 476-489.
40
- 41 [25] Sahraei, E., Hill, R., Wierzbicki, T., 2012a. "Calibration and Finite Element Simulation of Pouch
42 Lithium-Ion Batteries for Mechanical Integrity". *Journal of Power Sources*, 201, pp. 307-321.
43
- 44 [26] Sahraei, E., Kahn, M., Meierc J., Wierzbicki, T., 2015. "Modelling of Cracks Developed in
45 Lithium-Ion Cells under Mechanical Loading". *Royal Society of Chemistry Advances*, 5:80369.
46
- 47 [27] Sahraei, E., Wierzbicki, T., Hill, R., Luo, M., 2010. "Crash Safety of Lithium-ion Batteries towards
48 Development of a Computational Model". *SAE Technical Paper 2010-01-1078*, Detroit, Michigan
49 USA, April 13- April 15, 2010.
50
- 51 [28] Sahraei, E., Campbell, J., Wierzbicki, T., 2012b. "Modeling and short circuit detection of 18650
52 Li-ion cells under mechanical abuse conditions". *Journal of Power Sources*, 220, pp. 360-372.
53
- 54 [29] Lopez, C., Jeevarajan, J., Mukherjee, P., 2015. "Characterization of Lithium-Ion Battery Thermal
55 Abuse Behavior Using Experimental and Computational Analysis". *Journal of Electrochemical Society*,
56 162, 10, pp. A2163-A2173.
57
58
59
60

- [30] Bazinski, S. J., and Wang, X., 2015. "Experimental Study on the Influence of Temperature and State-of-Charge on the Thermophysical Properties of an LFP Pouch Cell". *Journal of Power Sources*, 293, pp. 283–291.
- [31] Spinner, N. S., Mazurick, R., Brandon, A., Rose-Pehrsson, S. L., Tuttle, S.G., 2015b. "Analytical, Numerical and Experimental Determination of Thermophysical Properties of Commercial 18650 LiCoO₂ Lithium-Ion Battery". *Journal of the Electrochemical Society*, 162(14), pp. A2789–A2795.
- [32] Siguang, L., and Chengning, Z., 2009. "Study on Battery Management System and Lithium-ion Battery". *Proceedings of IEEE, International Conference on Computer and Automation Engineering (ICCAE '09)*, 8-10 March 2009, Bangkok, Thailand.
- [33] Richardson, R. R., Ireland, P. T., Howey, D. A., 2014. "Battery Internal Temperature Estimation by Combined Impedance and Surface Temperature Measurement". *Journal of Power Sources*, 265, pp. 254–261.
- [34] Chen, Y., Evans, J.W., 1996. "Thermal analysis of Lithium-Ion batteries". *Journal of Electrochemical Society*, 143, pp. 2708–2712.
- [35] Kim, G.H., Pesaran, A., 2009. *Fifth International Symposium on Large Lithium Ion Battery Technology and Application*. June 9-10, 2009, Long Beach Convention Center, Long Beach, California, CA.
- [36] Marcicki, J., Zhu, M., Bartlett, A., Yang, X.G., Chen, Y., Miller, T., L'Eplattenier, P., Caldichoury, I., 2017. "A Simulation Framework for Battery Cell Impact Safety Modeling Using LS-DYNA". *Journal of the Electrochemical Society*, 164(1), pp. A6440-A6448.
- [37] Wang, W.W., YANG, S., Lin, C., 2016. "Clay-like Mechanical Properties of Components for the Jellyroll of Cylindrical Lithium-ion Cells". *Energy Procedia*, 104, pp. 56 – 61.
- [38] Xia, Y., Wierzbicki, T., Sahraei, E., Zhang, X., 2014. "Damage of Cells and Battery Pack due to Ground Impact". *Journal of Power Sources*, 267, pp. 78-97.
- [39] Trattng, G. and Leitgeb, W., 2014. "Battery Modelling for Crash Safety Simulation". *Virtual Vehicle Research Center, Graz, Austria, Automotive Engineering. Simulation and Validation Methods*, DOI: 10.1007/978-3-319-02523-0_2.
- [40] Wierzbicki, T., Sahraei, E., 2016. "Homogenized mechanical properties for the jellyroll of cylindrical Lithium-ion cells". *Journal of Power Sources*, 241, pp. 467-476.
- [41] Martínez-Rosas, E., Vasquez-Medrano, R., Flores-Tlacuahuac, A., 2011. "Modeling and Simulation of Lithium-Ion Batteries". *Computers and Chemical Engineering*, 35, pp. 1937–1948.
- [42] Xu, J., Liu, B., Hu, D., 2016. "State of Charge Dependent Mechanical Integrity Behavior of 18650 Lithium-ion Batteries". *Scientific Reports* 6, 21829; doi: 10.1038/srep21829 (2016).
- [43] "Material selector for LS-DYNA, 20162. LSTC website, <http://www.lstc.com/dynamat/>. (Accessed on June 2016).
- [44] Slik, G., Vogel, G., Chawda, V., 2006. "Material Model Validation of a High Efficient Energy Absorbing Foam". 5th LS-DYNA forum, 12-13 October 2006, Ulm, Germany.
- [45] Sheikh, M., Rehman, S., Elkady, M., Numerical simulation model for short circuit prediction under compression and bending of 18650 cylindrical lithium-ion battery, *Energy Procedia* (2018) 151 187-193.

1
2
3 [46] “LS-DYNA keyword user's manual, volume (ii) material models, LSTC, LS-DYNA R8.0”.
4 <http://www.dynasupport.com/manuals/ls-dyna-manuals/ls-dyna-manual-r-8.0-vol-ii>. (Accessed June
5 2016).
6

7 [47] The Engineering tool box, 2017. http://www.engineeringtoolbox.com/young-modulus-d_417.html
8 (Accessed on May 2017)
9

10 [48] Zhang, C., Santhanagopalan, S., Sprague, M.A., Pesaran, A.A., 2015a. “Coupled Mechanical-
11 Electrical-Thermal Modeling for Short-Circuit Prediction in a Lithium-Ion Cell under Mechanical
12 Abuse”. Journal of Power Sources, 290, pp. 102–113.
13

14 [49] Zhang, C., Santhanagopalan, S., Sprague, M.A., Pesaran, A.A., 2015b. “A Representative-
15 Sandwich Model for Simultaneously Coupled Mechanical-Electrical-Thermal Simulation of a Lithium-
16 Ion Cell under Quasi-Static Indentation Tests”. Journal of Power Sources, 298, pp. 309–321.
17

18 [50] Sahraei, E., Meier, J., Wierzbicki, T., 2014. “Characterizing and Modeling Mechanical Properties
19 and Onset of Short Circuit for Three Types of Lithium-Ion Pouch Cells”. Journal of Power Sources,
20 247, pp. 503–516.
21

22 [51] “LS-DYNA Consistent units”. LS-DYNA Support, 2017.
23 <http://www.dynasupport.com/howtos/general/consistent-units>
24 (Accessed January 2017).
25

26 [52] Nadimpalli, S.P.V., Sethuraman, V.A., Abraham, D.P., Bower, A.F., Guduru, P.R., 2015. “Stress
27 Evolution in Lithium-Ion Composite Electrodes during Electrochemical Cycling and Resulting Internal
28 Pressures on the Cell Casing”. Journal of the Electrochemical Society, 162(14), pp. A2656-A2663.
29

30 [53] Croop B., and Lobo, H., 2009. “Selecting Material Models for the Simulation of Foams in LS-
31 DYNA”. 7th European LS-DYNA Conference, 2009. DYNAmore GmbH.
32
33
34
35
36
37
38
39
40
41
42
43
44
45
46
47
48
49
50
51
52
53
54
55
56
57
58
59
60